

# Nonisothermal crystallization behaviour of poly( $\rho$ -dioxanone) and poly(L-lactic acid) blends

XIAOJIN ZHANG<sup>1,2</sup>, WEI BAI<sup>1,3,\*</sup>, DONGLIANG CHEN<sup>1,3</sup>, CHENGDONG XIONG<sup>1,3</sup> and XIUBING PANG<sup>3</sup>

<sup>1</sup>Chengdu Institute of Organic Chemistry, Chinese Academy of Sciences, Chengdu 610041, People's Republic of China

<sup>2</sup>University of Chinese Academy of Sciences, Beijing 100039, People's Republic of China

<sup>3</sup>Zhejiang Engineering Research Center in Biodegradable Medical Materials, Dongyang 322100, People's Republic of China

MS received 24 February 2014; revised 11 May 2014

**Abstract.** Blends of poly( $\rho$ -dioxanone) (PPDO) and poly(L-lactic acid) (PLLA) in different proportions were prepared by solution co-precipitation. The nonisothermal crystallization behaviour of pure PPDO and PPDO/PLLA blends was investigated by differential scanning calorimetry. The Avrami, Ozawa and Mo models were used to analyse the nonisothermal kinetics. The addition of PLLA significantly increases the crystallization peak temperature and crystallinity of PPDO, but has little effect on crystallization half-time. The activation energies of crystallization were calculated using the Kissinger equation. The results suggest that PLLA plays two roles in the nonisothermal crystallization of PPDO; PLLA both promotes the crystallization of PPDO as a nucleating agent and meanwhile restricts the motion of PPDO chains.

**Keywords.** Poly(L-lactide); poly( $\rho$ -dioxanone); blends; nonisothermal crystallization.

## 1. Introduction

Poly( $\rho$ -dioxanone) (PPDO) is a useful biomaterial due to its biodegradability and good mechanical properties.<sup>1–14</sup> It is already being used in some biological and medical applications, especially surgery repair materials such as sutures, bone repair devices, and drug delivery systems.<sup>15–17</sup> Like other aliphatic polyesters, however, it has a low crystallization rate and low melt strength. These characteristics of PPDO make it difficult to use in the production of thin clips and sutures by injection molding or extrusion molding, which hinders the development of PPDO as a promising future biomedical material.

Among the methods employed to enhance crystallization rates of polymers, introducing additives as nucleating agents is the most convenient and most frequently chosen strategy.<sup>8,9,18–20</sup> Poly(L-lactic acid) (PLLA), another linear aliphatic polyester, is considered to be one of the most promising materials because it can be made from agricultural products and is readily biodegradable. However, PLLA has poor flexibility, limiting its application. The blending of polymers has proven to be an excellent strategy for developing new materials; the blended compounds often exhibit combinations of properties superior to either of the individual components.<sup>21,22</sup> Compared to chemical modification, blending polymers represents a more cost-effective way to modify polymer properties.<sup>23</sup>

Blending PPDO with PLLA has been identified as a conceivable approach to combine the merits of these two polymers. Pezzin *et al*<sup>24</sup> and Pezzin and Duek<sup>25</sup> prepared blends of PPDO and PLGA by fusion and studied their properties. The interfacial damage properties of plasma-treated biodegradable PPDO fibre/PLLA composites were nondestructively evaluated by Park *et al*<sup>26</sup> using micromechanical testing and surface wettability measurements. To the best of our knowledge, all existing reports on PPDO/PLLA blends are related to their thermal, mechanical, morphological, interfacial and degradation properties; they do not include investigations of crystallization behaviour, one of the most dominant factors<sup>27–29</sup> that affects biomaterial properties and determines their applicability.

In this work, we report for the first time the effect of PLLA on the nonisothermal crystallization behaviour of PPDO. Blends of PPDO and PLLA in different proportions were prepared by solution co-precipitation. Several kinetic models were applied to analyse the crystallization kinetics, and the effective activation energy was calculated by the Kissinger equation. The investigation of the nonisothermal crystallization kinetic properties of PPDO/PLLA blends in this work contributes to the understanding of their crystallization behaviours.

## 2. Experimental

### 2.1 Materials

PPDO (Chengdu Organic Chemistry Company) was prepared by molten state ring-opening copolymerization in

\*Author for correspondence (baiwei@cioc.ac.cn)

using stannous octoate as an initiator under high vacuum. PLLA (Chengdu Organic Chemistry Company) was prepared according to the same protocol under high purity nitrogen. The measured intrinsic viscosity of PPDO in hexafluoroisopropanol (Sigma Aldrich) was  $2.01 \text{ dl g}^{-1}$ . The measured intrinsic viscosity of PLLA in chloroform (Guangdong Guanghua Chemical Factory Co. Ltd) was  $2.63 \text{ dl g}^{-1}$ . Ethanol (Guangdong Guanghua Chemical Factory Company) and hexafluoroisopropanol were analytical grade and used as-received.

## 2.2 Blend preparation

Prior to use, PPDO and PLLA were dried under vacuum for 24 h at  $30^\circ\text{C}$ . The mass ratios of PPDO to PLLA were fixed at 100/0, 95/05, 90/10, 85/15, 70/30 and 60/40. PPDO/PLLA composites were prepared by solution coprecipitation; PPDO was dissolved in hexafluoroisopropanol and added to a solution of PLGA in chloroform. The mixture was subjected to ultrasonic agitation for 4 h to ensure complete mixing. Excess ethanol was then added to the mixture to separate the composites from the solvent. Upon removal of the solvent, the PPDO/PLLA composites were obtained and dried to constant weights under vacuum at  $30^\circ\text{C}$ .

## 2.3 DSC characterization

Differential scanning calorimetry (DSC) measurements (Q2000; American TA Company Instruments) were obtained under nitrogen atmosphere. The temperature was calibrated with indium. Samples (4–5 mg) were enclosed in aluminum pans; an empty aluminum pan was used as a reference. For nonisothermal analysis, samples were first held at  $140^\circ\text{C}$  for 5 min to erase thermal history. The samples were subsequently cooled to  $-10^\circ\text{C}$  at cooling rates of 5, 15, 30 and  $50^\circ\text{C min}^{-1}$ , and the exothermic curves were recorded.

## 3. Results and discussion

### 3.1 Nonisothermal crystallization behaviour of PPDO/PLLA blends

The nonisothermal crystallization exotherms of PPDO/PLLA blends (100/0, 95/05, 90/10, 85/15, 70/30 and 60/40) at different cooling rates are presented in figure 1. The crystallization peak temperature ( $T_p$ ), onset temperature ( $T_o$ ), and crystallization enthalpy ( $\Delta H_C$ ) of the blends are listed in table 1. A decrease in  $T_o$  and  $T_p$  along with the broadening of the exothermal peak is observed with increasing cooling rate, indicating that crystallization occurs at higher temperatures for lower cooling rates. This result can be explained by the fact that PPDO molecules are able to better arrange themselves at lower cooling rates; therefore, less supercooling is required to initiate the crystallization of PPDO at lower cooling rates.

The  $T_o$  and  $T_p$  of PPDO/PLLA blends are shifted to higher temperatures compared to those of pure PPDO, indicating that PLLA behaves as a nucleating agent for the crystallization of PPDO. Among the PPDO/PLLA blends with different proportions, the  $T_p$  of the 85/15 blend is the highest. This can be attributed to two factors. First, the number of nucleation sites increases with increasing PLLA content, which facilitates the crystallization of PPDO. Second, increasing PLLA content introduces more steric hindrance, limiting the mobility of PPDO chains. On the other hand, the  $\Delta H_C$  of PPDO/PLLA blends are higher than that of pure PPDO for a given cooling rate, suggesting that PLLA enhances PPDO's total crystallinity ( $X_t$ ):

$$X_t = \frac{\int_{T_0}^T (dH/dT) dT}{\int_{T_0}^{T_\infty} (dH/dT) dT}, \quad (1)$$

where  $T_0$  and  $T_\infty$  represent the initial and end crystallization temperatures, respectively and  $dH/dT$  the heat flow rate. For nonisothermal crystallization, the time  $t$  and temperature  $T$  have the following relation:

$$t = \frac{T_0 - T}{\varphi}, \quad (2)$$

where  $\varphi$  is the cooling rate and  $T$  the crystallization temperature at time  $t$ .

Figure 2 shows the changes in the relative crystallinity of PPDO/PLLA blends as a function of time. The crystallization half-time values  $t_{1/2}$  of all blends are also listed in table 1. The addition of PLLA only slightly decreases the  $t_{1/2}$  value of pure PPDO, which can be explained by the contradictory effects of the  $\pi$ - $\pi$  interaction between PPDO and PLLA on polymer crystallization. On the one hand, the  $\pi$ - $\pi$  interaction induces the orientation of PPDO chains along PLLA domains, prompting the crystallization of PPDO. On the other hand, the  $\pi$ - $\pi$  interaction restricts the migration and diffusion of PPDO chains, suppressing PPDO crystallization. For solution crystallization processes, especially in dilute solutions, crystallization is dominated by nucleation processes because the diffusion of PPDO chains is weak. However, for melt crystallization processes, the contribution of nucleation to the total crystallization rate is greatly impaired by the restriction effect.

### 3.2 Kinetic analysis by the Avrami model

The Avrami model for the analysis of the nonisothermal crystallization kinetics of PPDO/PLLA blends can be expressed by the following equations:<sup>30,31</sup>

$$1 - X_t = \exp(-Kt^n), \quad (3)$$

$$\ln[-\ln(1 - X_t)] = \ln K + n \ln t, \quad (4)$$

where  $n$  is the Avrami exponent that depends on nucleation and growth during crystallization and  $K$  the

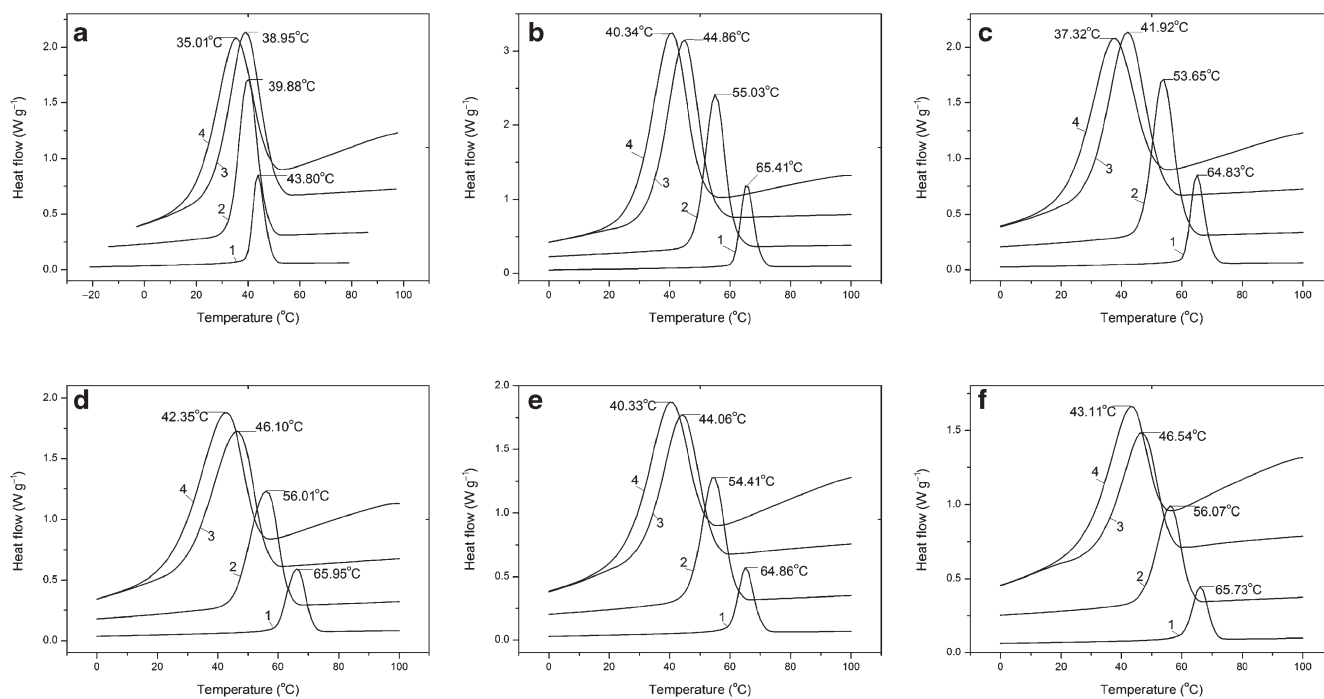


**Figure 1.** Differential scanning calorimetry exothermal curves of nonisothermal crystallization with different cooling rates for PPDO/PLLA blends: (a) PPDO/PLLA100/0; (b) PPDO/PLLA95/05; (c) PPDO/PLLA90/10; (d) PPDO/PLLA85/15; (e) PPDO/PLLA70/30 and (f) PPDO/PLLA60/40, (1) cooling rate: 5°C min<sup>-1</sup>; (2) cooling rate: 15°C min<sup>-1</sup>; (3) cooling rate: 30°C min<sup>-1</sup>; (4) cooling rate: 50°C min<sup>-1</sup>.

**Table 1.** Nonisothermal crystallization kinetic parameters for all samples.

Sample	$\varphi$ (°C min <sup>-1</sup> )	$T_0$ (°C)	$T_p$ (°C)	$t_{1/2}$ (min)	$\Delta H_C$ (J g <sup>-1</sup> )	$n$	$K_C$
PPDO/PLLA100/0	5	53.51	43.80	2.81	17.32	3.82	0.5096
	15	52.39	39.88	1.72	15.87	4.26	0.9223
	30	51.70	38.95	1.17	14.88	3.40	0.9557
	50	50.74	35.01	0.91	14.02	3.52	1.0109
PPDO/PLLA95/05	5	70.04	65.41	2.52	73.18	5.48	0.4910
	15	61.31	55.03	1.29	69.43	4.30	0.8951
	30	53.87	44.86	0.84	64.67	4.31	1.0078
	50	50.52	40.34	0.70	60.77	3.29	1.0290
PPDO/PLLA90/10	5	69.82	64.83	2.12	54.40	4.63	0.5053
	15	60.85	53.65	1.27	50.49	4.44	0.9841
	30	53.40	41.92	0.81	46.76	3.99	1.0098
	50	50.30	37.32	0.68	41.80	3.35	1.0187
PPDO/PLLA85/15	5	71.46	65.95	1.95	45.39	3.99	0.5291
	15	63.35	56.10	1.19	43.13	3.93	0.8774
	30	56.35	46.81	0.74	39.09	3.92	1.0093
	50	53.13	42.35	0.49	36.06	2.47	1.0255
PPDO/PLLA70/30	5	70.35	64.85	2.11	38.78	4.73	0.5369
	15	61.53	54.41	1.28	37.40	4.34	0.8447
	30	54.41	44.06	0.77	34.61	3.83	1.0183
	50	51.37	40.33	0.63	31.47	2.89	1.0266
PPDO/PLLA60/40	5	70.94	65.73	1.97	27.51	3.94	0.5157
	15	62.86	56.07	1.17	25.74	5.02	0.8606
	30	55.95	46.54	0.68	23.60	3.94	1.0322
	50	52.80	42.11	0.44	21.73	4.64	1.0388

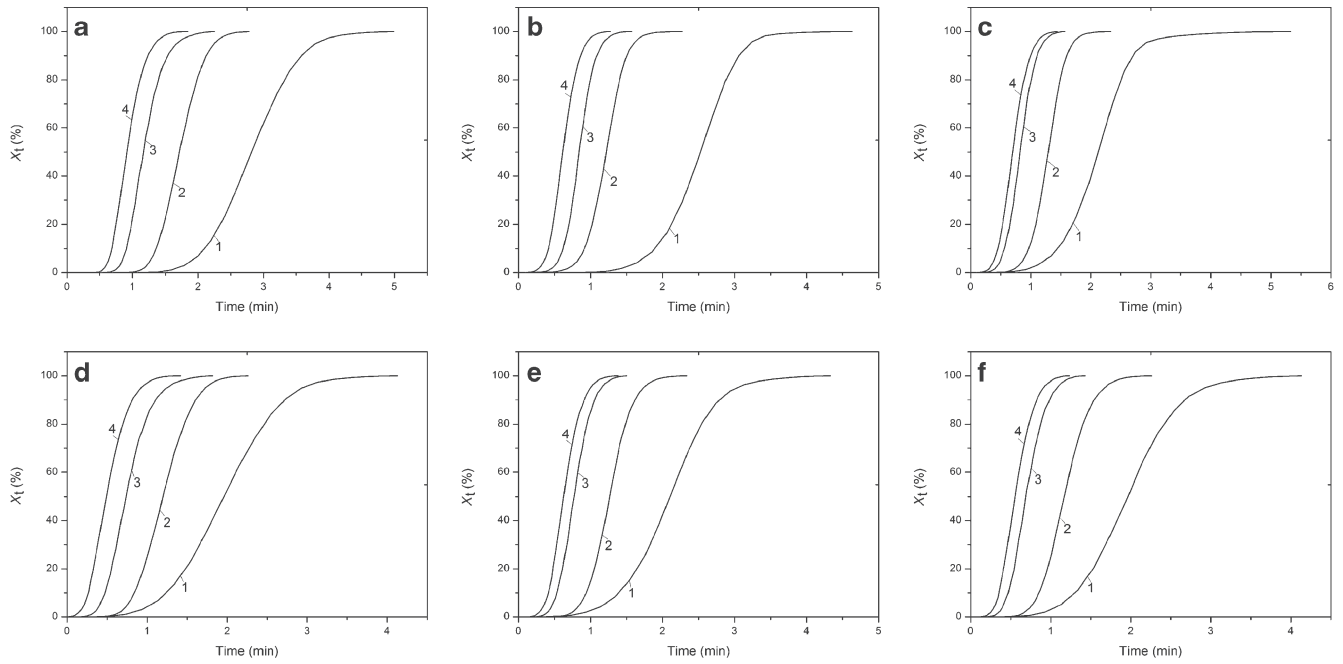


**Figure 2.** Plots of relative crystallization as a function of time ( $t$ ) at different cooling rates for pure PPDO and PPDO/PLLA blends: (a) PPDO/PLLA100/0; (b) PPDO/PLLA95/05; (c) PPDO/PLLA90/10; (d) PPDO/PLLA85/15; (e) PPDO/PLLA70/30 and (f) PPDO/PLLA60/40, (1) cooling rate:  $5^{\circ}\text{C min}^{-1}$ ; (2) cooling rate:  $15^{\circ}\text{C min}^{-1}$ ; (3) cooling rate:  $30^{\circ}\text{C min}^{-1}$ ; (4) cooling rate:  $50^{\circ}\text{C min}^{-1}$ .

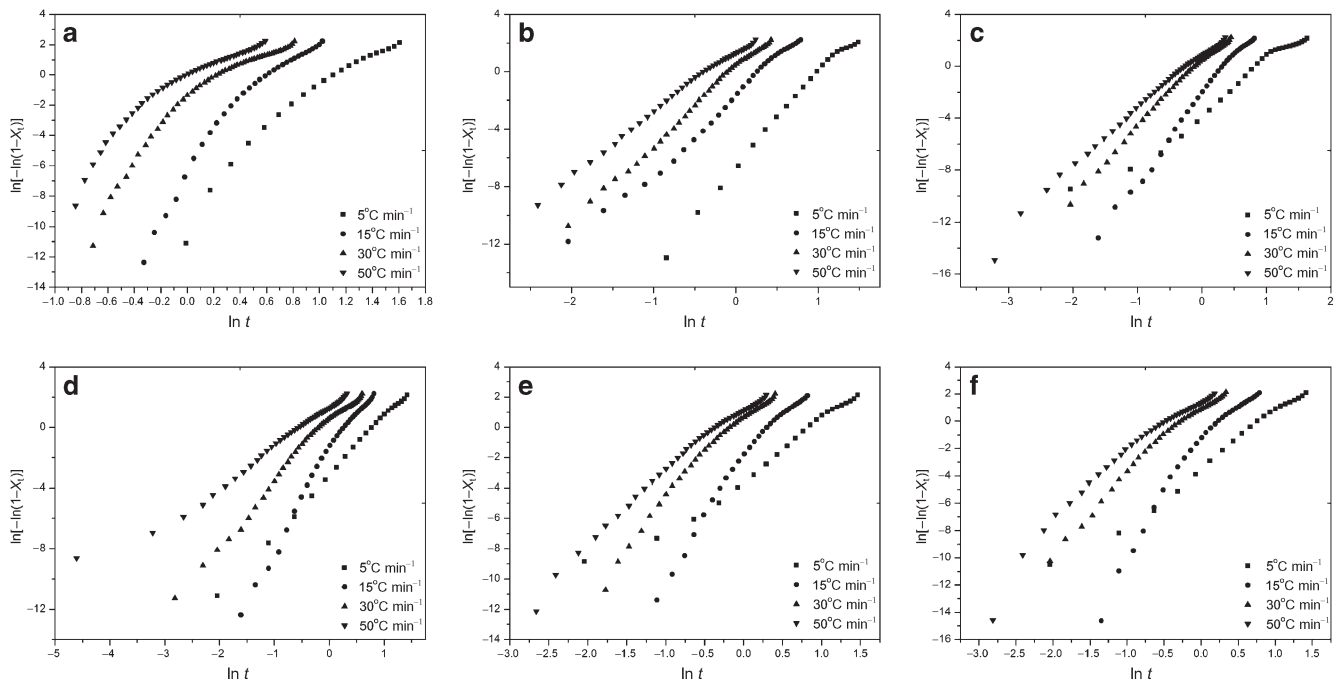


**Figure 3.** Plots of  $\ln[-\ln(1-X_t)]$  vs.  $\ln t$  for pure PPDO and PPDO/PLLA blends: (a) PPDO/PLLA100/0; (b) PPDO/PLLA95/05; (c) PPDO/PLLA90/10; (d) PPDO/PLLA85/15; (e) PPDO/PLLA70/30 and (f) PPDO/PLLA60/40.

temperature-dependent rate constant. Assuming a constant cooling rate  $\varphi$  in the nonisothermal process, Jeziorny<sup>32</sup> gave the corrected form of  $K$  as follows:

$$\ln K_C = \frac{\ln K}{\varphi}. \quad (5)$$

Figure 3 presents plots of  $\ln[-\ln(1-X_t)]$  vs.  $\ln t$  for PPDO/PLLA blends. The values of the Avrami exponent  $n$  and the rate constant  $K$  or  $K_C$  are obtained from the slope and intercept of the linear region of these plots.<sup>33</sup> Because the middle portion of the curves represent 15–70% of the crystallization process, the  $n$ ,  $K$  and  $K_C$  values are adopted from

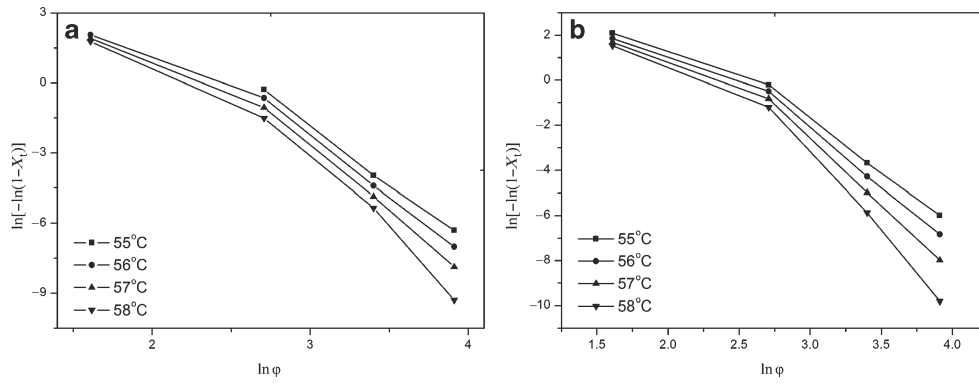


**Figure 4.** Ozawa plots of  $\ln[-\ln(1-X_t)]$  vs.  $\ln \phi$  at indicated temperatures for pure PPDO and PPDO/PLLA blends: (a) PPDO/PLLA100/0; (b) PPDO/PLLA95/05; (c) PPDO/PLLA90/10; (d) PPDO/PLLA85/15; (e) PPDO/PLLA70/30 and (f) PPDO/PLLA60/40.

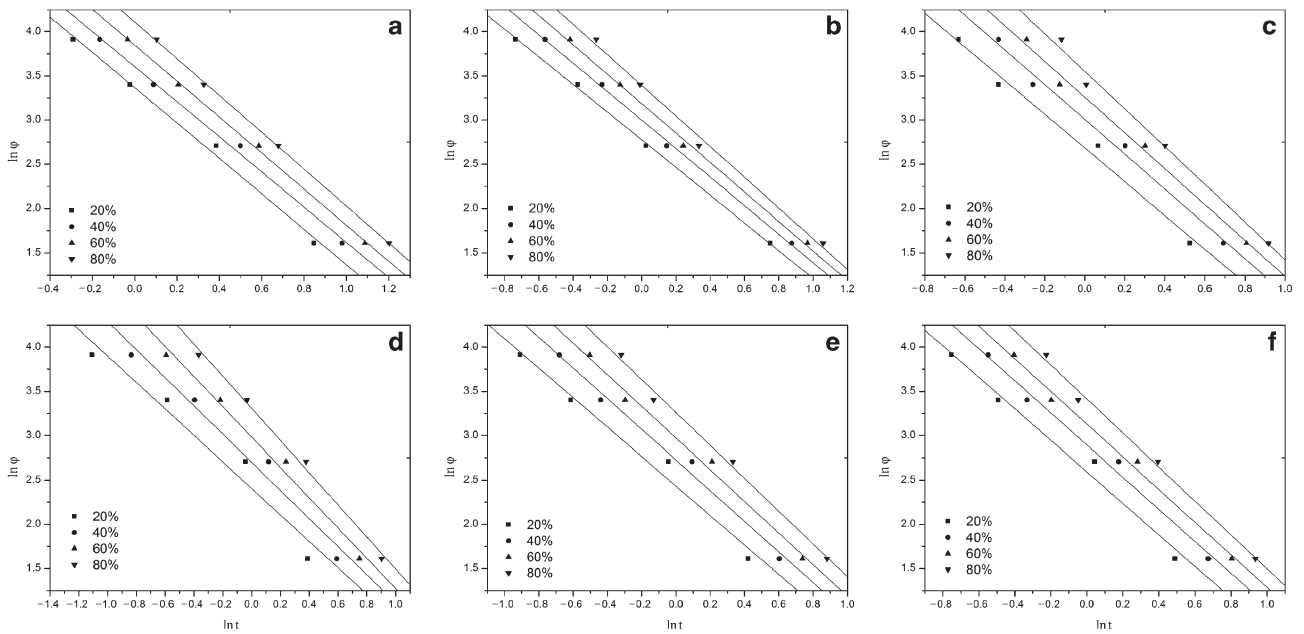


**Figure 5.** Plots of  $\ln \phi$  vs.  $\ln t$  for the nonisothermal crystallization of pure PPDO and PPDO/PLLA blends: (a) PPDO/PLLA100/0; (b) PPDO/PLLA95/05; (c) PPDO/PLLA90/10; (d) PPDO/PLLA85/15; (e) PPDO/PLLA70/30 and (f) PPDO/PLLA60/40.

**Table 2.** Values of  $\alpha$  and  $F(T)$  for PPDO/PLLA blends.

Sample	Parameters	$X_t\%$			
		20	40	60	80
PPDO/PLLA100/0	$\alpha$	1.9995	1.9853	2.03464	2.0813
	$F(T)$	28.9569	36.7398	46.8439	60.9053
PPDO/PLLA95/05	$\alpha$	1.5646	1.6097	1.6633	1.7308
	$F(T)$	16.0569	20.2208	27.3318	34.8360
PPDO/PLLA90/10	$\alpha$	1.9054	1.9667	2.0223	2.1288
	$F(T)$	14.8927	20.0592	25.9848	30.3774
PPDO/PLLA85/15	$\alpha$	1.5874	1.7083	1.8136	1.4939
	$F(T)$	14.6320	19.7622	24.1615	29.7019
PPDO/PLLA70/30	$\alpha$	1.7785	1.8128	1.8442	1.91807
	$F(T)$	15.3505	21.0721	24.8781	30.0802
PPDO/PLLA60/40	$\alpha$	1.6639	1.7303	1.7869	1.8547
	$F(T)$	15.3683	22.2589	26.5476	31.0761

these portions (table 1). The values of  $n$  range from 3.40 to 4.26 for pure PPDO and 2.47 to 5.48 for the blends. The  $n$  values are nonintegers that sometimes exceed 4, which suggests a complicated crystallization mechanism. The values of  $K_C$  associated with nucleation and growth rates are comparable for pure PPDO and blends. They suggest that the incorporation of PLLA does not significantly change the nonisothermal crystallization rates of PPDO due to competition between the nucleation and restriction effects.

### 3.3 Kinetic analysis based on the Ozawa model

Considering the nonisothermal crystallization to be a cooling rate-dependent process, Ozawa<sup>34</sup> presented an extended Avrami model

$$1 - X_t = \exp[-Z(T)/\varphi^m], \quad (6)$$

where  $Z(T)$  is the crystallization rate constant and  $m$  the Ozawa exponent. Equation (6) can be rearranged into a logarithmic form

$$\ln[-\ln(1 - X_t)] = \ln Z(T) - m \ln \varphi. \quad (7)$$

The plots of  $\ln[-\ln(1 - X_t)]$  vs.  $\ln \varphi$  for pure PPDO and 95/05 PDDO/PLLA blends are shown in figure 4. A series of straight lines in figure 4 would indicate that the Ozawa model can correctly describe the nonisothermal crystallization kinetics, and  $Z(T)$  and  $m$  could be determined from the intercept and the slope, respectively. However, no such straight lines for pure PPDO and 95/05 blends are observed, meaning that the Ozawa model fails to effectively describe the nonisothermal crystallization of pure PPDO and polymer blends. The reason for this may be that secondary crystallization occurred as a melt crystallization processes, which is not considered in the Ozawa model.

### 3.4 Kinetic analysis based on the Mo model

Because both the Avrami and Ozawa models do not effectively describe the nonisothermal crystallization of polymer melts, the model of Liu *et al.*,<sup>35</sup> which combines the Avrami and Ozawa models, was employed

$$\ln K + n \ln t = \ln Z(T) - m \ln \varphi, \quad (8)$$

$$\ln \varphi = \ln F(T) - \alpha \ln t, \quad (9)$$

where  $\alpha$  is the ratio of the Avrami exponent  $n$  to the Ozawa exponent  $m$  and the parameter  $F(T) = [Z(T)/K]^{1/m}$  indicates the cooling rate when the system reaches a certain degree of crystallinity in unit time.  $F(T)$  has a definite physical implication; higher values of  $F(T)$  correspond to slower crystallization rates. Plots of  $\ln \varphi$  vs.  $\ln t$  at different degrees of crystallinity are shown in figure 5. The linearity of these plots suggests that this improved model is valid for describing the nonisothermal crystallization of pure PPDO and PPDO/PLLA blends.

The parameter  $F(T)$  and  $\alpha$  are listed in table 2; it can be seen that  $\alpha$  values change little with crystallinity, while  $F(T)$

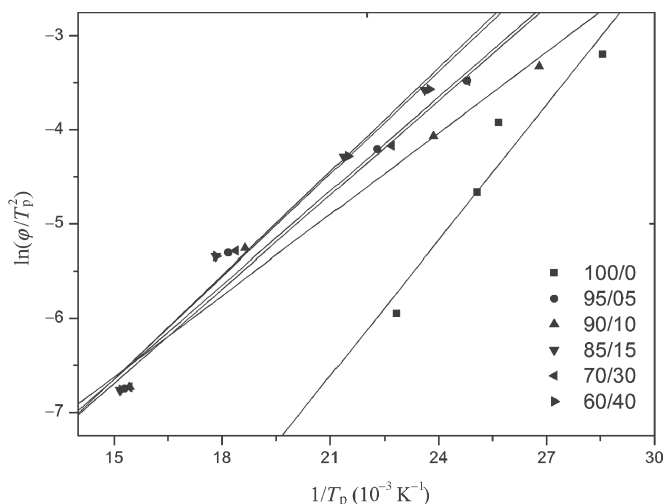


**Figure 6.** Plots of  $\ln(\varphi/T_p^2)$  vs.  $1/T_p$  for pure PPDO and PPDO/PLLA.

**Table 3.**  $\Delta E$  values of pure PPDO and PPDO/PLLA blends.

PPDO/PLLA	$\Delta E$ (kJ mol <sup>-1</sup> )
100/0	3.99
95/05	2.77
90/10	2.39
85/15	2.22
70/30	2.87
60/40	3.02

increases with increase in the relative crystallinity for all samples. In response to increasing PLLA content, the  $F(T)$  of blends first decreases for PLLA contents in PPDO ranging from 5 to 15%, but then increases upon further increase in the percentage of PLLA. This result suggests that a large PLLA content lowers the crystallization rate. As aforementioned, PLLA significantly suppresses the chain diffusion of PPDO due to the strong  $\pi$ - $\pi$  interaction between PPDO and PLLA.

### 3.5 Crystallization activation energy

For nonisothermal crystallization, the activation energy can be derived from the crystallization peak temperature ( $T_p$ ) and cooling rate ( $\varphi$ ) by the Kissinger<sup>36</sup> equation:

$$\frac{d(\ln(\varphi/T_p^2))}{d(1/T_p)} = -\frac{\Delta E}{R}, \quad (10)$$

where  $R$  is the gas constant and  $\Delta E$  the activation energy, which is composed of the transport activation energy  $\Delta E^*$  and the nucleation activation energy  $\Delta F$  and related to the energy barrier to polymer segments moving toward the growing front of a crystal. Figure 6 shows plots of  $\ln(\varphi/T_p^2)$  vs.  $1/T_p$  for pure PPDO and PPDO/PLLA blends, and the activation energies are listed in table 3. The values of  $\Delta E$  for all PPDO/PLLA blends are smaller than those obtained

for pure PPDO, implying that PLLA content can accelerate PPDO crystallization. Additionally,  $\Delta E$  is significantly decreased for the 95/05, 90/10 and 85/15 blends compared with pure PPDO, but is increased for the 70/30 and 60/40 blends compared with the above three blends. This suggests that the addition of 30% PLLA or above suppresses the motion of PPDO chains, and that the heterogeneous nucleation effect is not sufficient to offset the influence of the restriction effect; therefore, the  $\Delta E$  of the 70/30 and 60/40 blends is higher than that of the 95/05, 90/10 and 85/15 blends. The 85/15 blend exhibits a relatively low  $\Delta E$  due to the presence of more heterogeneous nucleation sites and a less-pronounced restriction effect.

#### 4. Conclusions

PPDO/PLLA blends with different PLLA contents were prepared *via* solution co-precipitation. Three kinetic models were used to analyse the nonisothermal crystallization behaviour of pure PPDO and blends. The Avrami and Ozawa models failed to effectively describe the behaviour, while the combined Avrami–Ozawa model proposed by Mo and coworkers accurately describes the crystallization process.

Compared with pure PPDO, the crystallization peak temperature and crystallinity of PPDO in blends is dramatically increased, although the change in crystallization half-time is slight. The activation energy determined by the Kissinger model first decreases and then increases with the increase in PLLA content, and  $\Delta E$  for all PPDO/PLLA blends is smaller than in pure PPDO. This is attributed to the increase in heterogeneous nucleation sites brought about by PLLA, which reduces the activation energy of PPDO in blends. The restriction effect of PLLA on PPDO, however, is increased, reducing the mobility of polymer chains when the PLLA content in PPDO is further increased.

#### Acknowledgements

This work was supported by grants from the National Natural Science Foundation of China (51103156) and the West Light Foundation of the Chinese Academy of Sciences.

#### References

1. Yang K K, Wang X L and Wang Y Z 2002 *J. Macromol. Sci. Polym. Rev.* **C42** 373
2. Nishida H, Yamoshita M, Endo T and Tokiwa Y 2000 *Macromolecules* **33** 6982
3. Huang H X, Yang K K, Wang Y Z, Wang X L and Jun L 2006 *J. Polym. Sci. A: Polym. Chem.* **44** 1245
4. Yoon K R, Lee K B, Chi Y S, Yun W S, Joo S W and Choi I S 2003 *Adv. Mater.* **15** 2063
5. Furuhashi Y, Nakayama A, Monno T, Kawahara Y, Yamane H, Kimura Y and Iwata T 2004 *Macromol. Rapid Commun.* **25** 1943
6. Sabino M A, Albuerne J, Muller A J, Brisson J and Prudhomme R E 2004 *Biomacromolecules* **5** 358
7. Yang K K, Wang X L, Wang Y Z and Huang H X 2004 *Mater. Chem. Phys.* **87** 218
8. Sabino M A, Feijoo J L and Muller A J 2000a *Macromol. Chem. Phys.* **201** 2687
9. Sabino M A, Ronca G and Muller A J 2000b *J. Mater. Sci.* **35** 5071
10. Chen S C, Wang X L, Wang Y Z, Yang K K, Zhou Z X and Wu G 2007 *J. Biomed. Mater. Res. A* **80A** 453
11. Wang X L, Yang K K, Wang Y Z, Wang D Y and Yang Z 2004 *Acta Mater.* **52** 4899
12. Zheng L, Wang Y Z, Yang K K, Wang X L, Chen S C and Li J 2005 *Eur. Polym. J.* **41** 1243
13. Bhattarai S R, Yi H K, Bhattarai N, Hwang P H and Kim H Y 2006 *Acta Biomater.* **2** 207
14. Bhattarai S R, Bhattarai N, Yi H K, Hwang P H, Cha D I and Kim H Y 2004 *Biomaterials* **25** 2595
15. Suzuki A, Terai H, Toyoda H, Namikawa T, Yokota Y, Tsunoda T and Takaoko K 2006 *J. Orthopaedic Res.* **24** 327
16. Toyoda H, Terai H, Sasaoka R, Oda K and Takaoko K 2005 *Bone* **37** 555
17. Yomeda M, Terai H, Imai Y, Okada T, Nozaki K, Inoue H, Miyamoto S and Takaoko K 2005 *Biomaterials* **26** 5145
18. Dong T, He Y, Zhu B, Shin K M and Inoue Y 2005 *Macromolecules* **38** 7736
19. Kai W H, He Y, Asakawa N and Inoue Y 2004 *J. Appl. Polym. Sci.* **94** 2466
20. Liu W J, Yang H L, Wang Z, Dong L S and Liu J 2002 *J. Appl. Polym. Sci.* **86** 2145
21. Pearce R and Marchessault R H 1994 *Polymer* **35** 3990
22. Vazquez-Torres H and Cruz-Ramos C A 1994 *J. Appl. Polym. Sci.* **54** 1141
23. Iannace S, Ambrosio L, Huang S J and Nicolais L 1994 *J. Appl. Polym. Sci.* **54** 1525
24. Pezzin A P T, Alberda E G, Zavaglia C A C, Brinke G and Duek E A R 2003 *J. Appl. Polym. Sci.* **88** 2744
25. Pezzin A P T and Duek E A R 2006 *J. Appl. Polym. Sci.* **101** 1899
26. Park J M, Kim D S and Kim S R 2004 *Comp. Sci. Tech.* **64** 847
27. Gilding D K and Reed A M 1979 *Polymer* **20** 1459
28. Anderson J M and Shive M S 1997 *Adv. Drug Deliv. Rev.* **28** 6
29. Eldsater C, Erlandsson B, Renstad R, Albertsson A and Karlsson S 2000 *Polymer* **41** 1297
30. Avrami J M 1940 *Chem. Phys.* **8** 212
31. Avrami J M 1941 *Chem. Phys.* **9** 1771
32. Jeziorny A 1978 *Polymer* **19** 1142
33. Weng W G, Chen G H and Wu D 2003 *Polymer* **44** 8119
34. Ozawa T 1971 *Polymer* **12** 150
35. Liu T X, Mo Z S and Zhang H F 1998 *J. Appl. Polym. Sci.* **67** 815
36. Kissinger H E 1956 *J. Res. Natl. Bur. Stand.* **57** 217